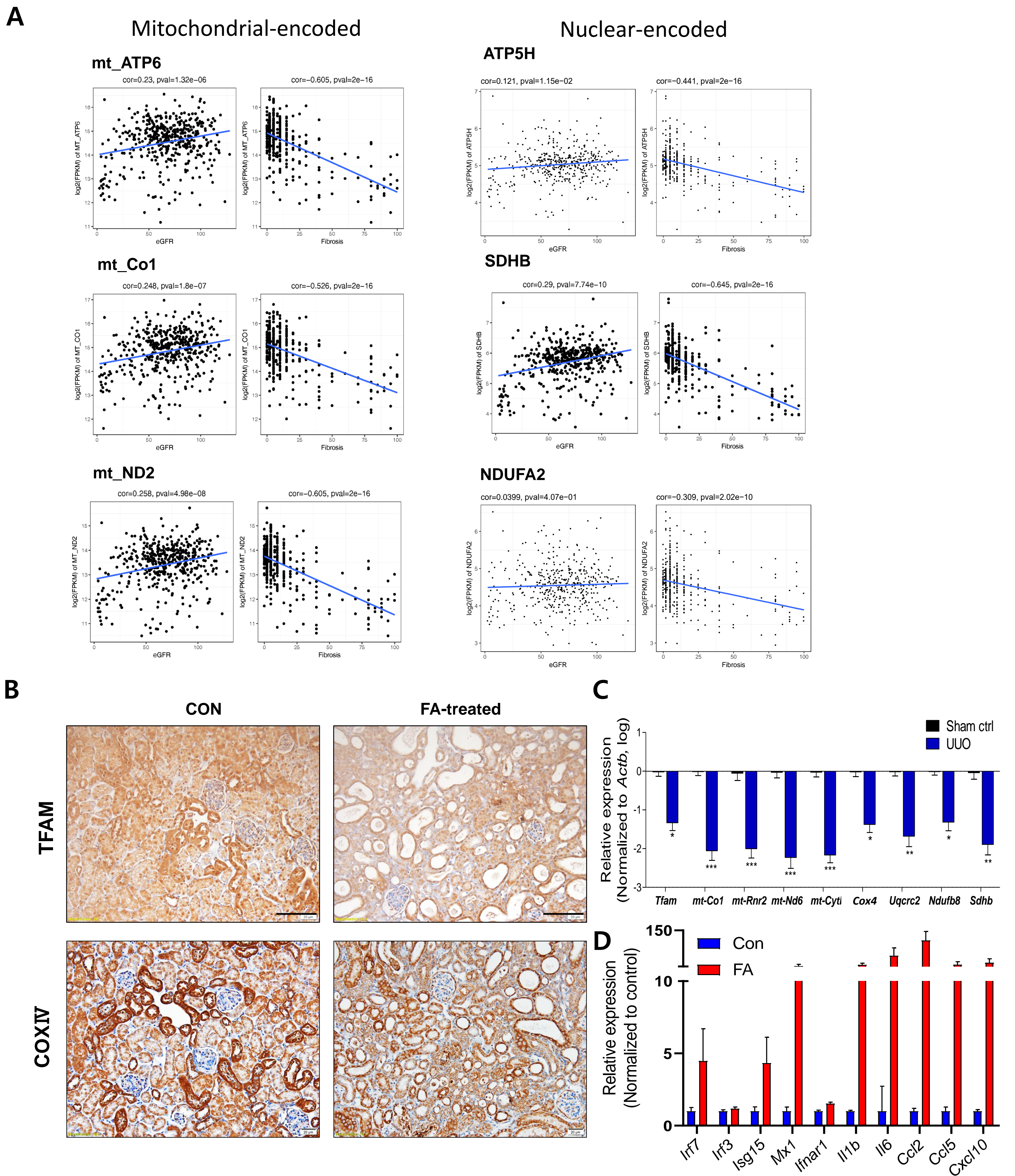
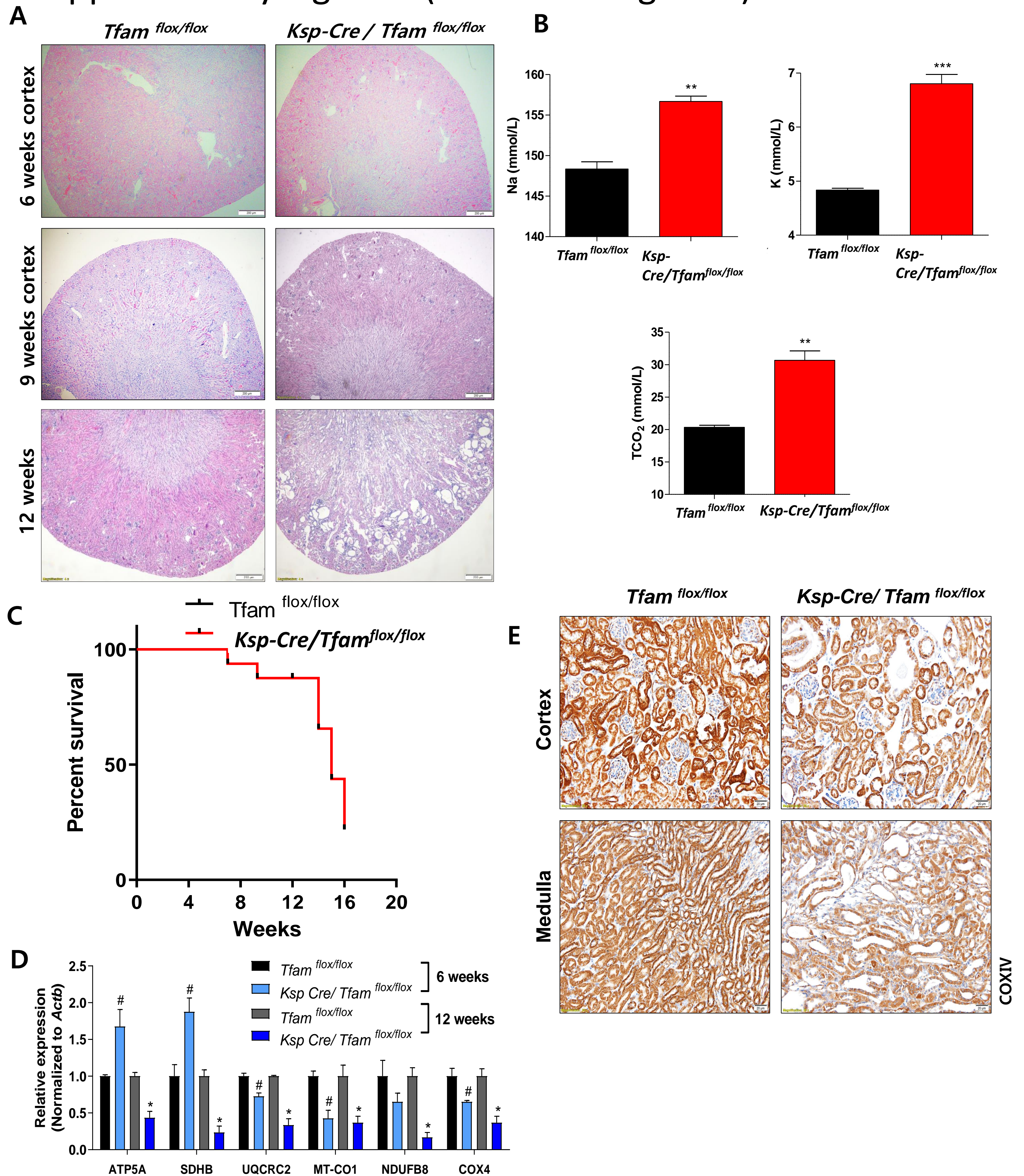


Supplementary Figure 1 (Related to Figure 1)



Supplementary Figure 1 (Related to Figure 1). Mouse and human kidney disease is characterized a decrease in and metabolic genes and increase in inflammatory genes. (A) Transcript level (RNAseq) of mitochondrial genes (*mtATP6*, *ATP5H*, *mtCO1*, *SDHB*, *mtND2*, *NDUFA2*) correlates with the degree of kidney fibrosis and kidney function (eGFR) of 433 microdissected human kidney samples. **(B)** TFAM and COXIV expressions in FA treated kidney fibrosis model were visualized by immunohistochemical (IHC) staining. Scale bar = 20 μ m. **(C)** Relative mRNA levels of *Tfam* and mitochondrial OXPHOS genes (*mt-Co1*, *mt-Rnr2*, *mt-Nd6*, *mt-Cytl*, *Cox4*, *Uqcrc2*, *Ndufb8*, and *Sdhb*) in folic acid (FA)-induced mice kidney fibrosis model. * $P < 0.05$, ** $P < 0.01$, *** $P < 0.001$ vs. Control. **(D)** Expression levels of IFN and proinflammatory genes (RNAseq) in FA-induced kidney fibrosis mice model.

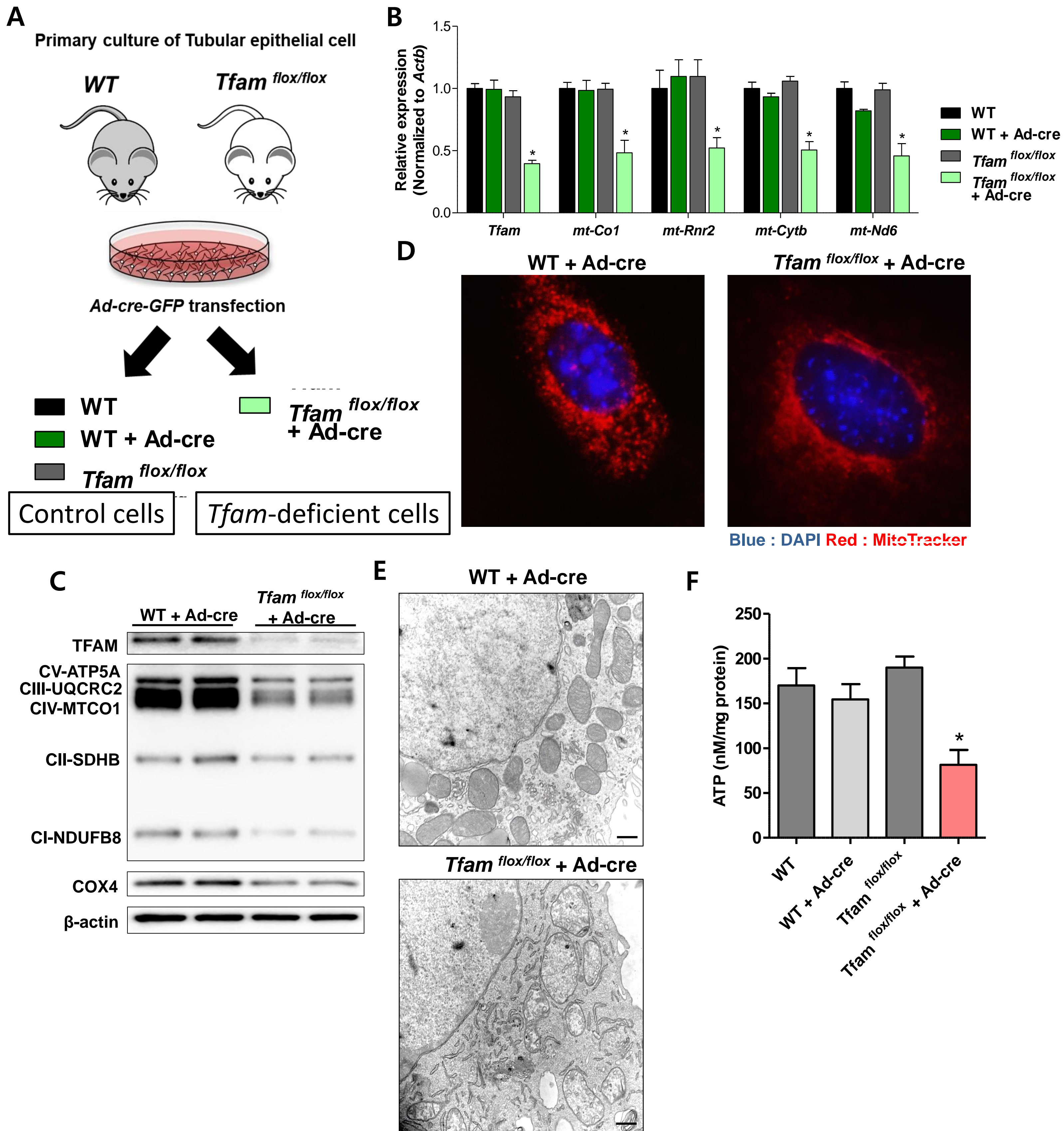
Supplementary Figure 2 (Related to Figure 2)



Supplementary Figure 2 (Related to Figure 2). Tubule specific TFAM deletion in mice causes renal failure.

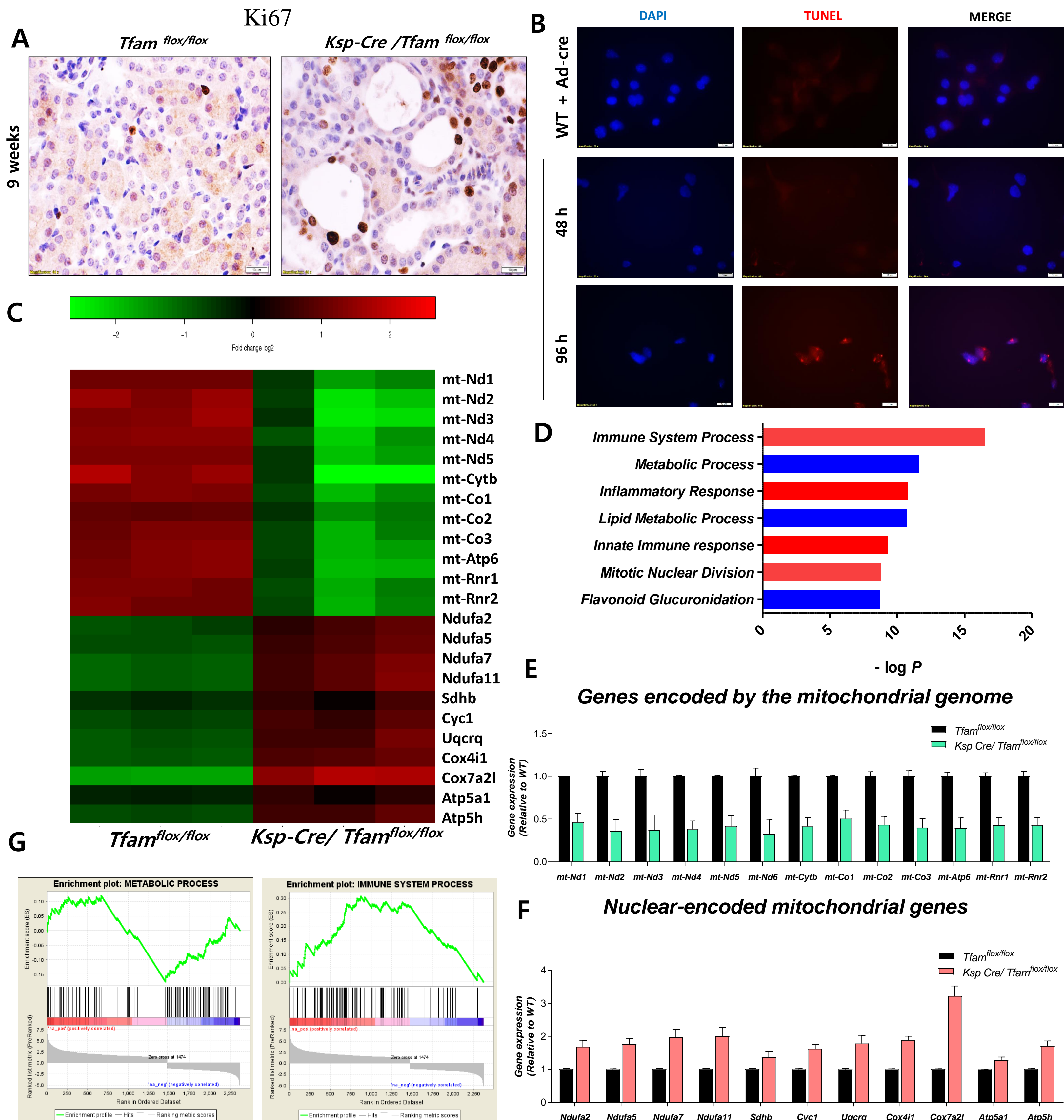
(A) Representative images of haematoxylin and eosin (H&E) staining of 6 weeks, 9 weeks and 12 weeks old *Ksp-Cre/Tfam*^{flox/flox} mice and WT/*Tfam*^{flox/flox} kidney. Scale bar = 200 μ m. (B) Blood sodium, potassium and total CO₂ levels in 12 weeks old *Ksp-Cre/Tfam*^{flox/flox} and WT/*Tfam*^{flox/flox} mice ****P* < 0.001. (C) Survival curve of *Ksp-Cre/Tfam*^{flox/flox} and WT/*Tfam*^{flox/flox} mice. (D) Relative protein levels (densitometry) of mitochondrial proteins (ATP5A, SDHB, UQCRC2, MT-CO1, NDUFB8, and COX4) in 6 weeks and 12 weeks of *Ksp-Cre/Tfam*^{flox/flox} mice and WT/*Tfam*^{flox/flox} mice kidney. * *P* < 0.05 vs. 6 weeks WT/*Tfam*^{flox/flox}. # *P* < 0.05 vs. 12 weeks WT/*Tfam*^{flox/flox}. (E) Representative immunostaining of COXIV of 12 weeks of *Ksp-Cre/Tfam*^{flox/flox} mice and WT/*Tfam*^{flox/flox} mice kidney.

Supplementary Figure 3 (Related to Figure 3)



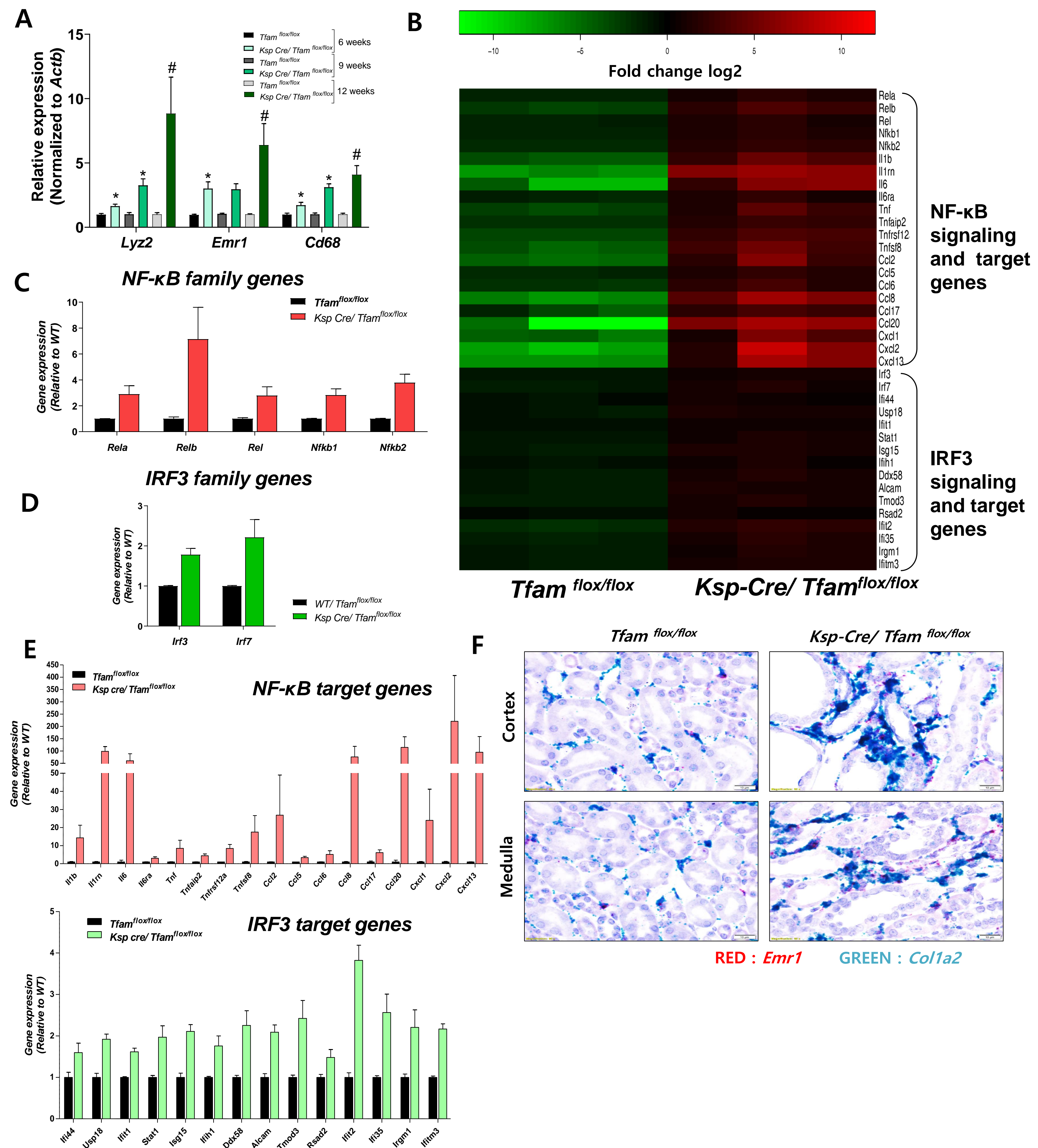
Supplementary Figure 3 (Related to Figure 3). *Tfam* deletion in primary tubule cells leads to severe metabolic defect
(A) Experimental design to generate control and *Tfam* knock-out TECs. Cells were cultured from wild type or *Tfam*^{flox/flox} mice and infected with Ad-Cre-GFP to generate control (wild type) and *Tfam*-deficient cells. **(B)** Relative transcript levels of mitochondrial genes expression of wild type cells and *Tfam*^{flox/flox} cells transfected with Ad-Cre-GFP. **(C)** Mitochondrial OXPHOS proteins expression in control and *Tfam* knock-out cells. **(D)** Representative images of control and *Tfam* knock-down TECs stained with DAPI and mitotracker. **(E)** Representative electron micrographs of control and *Tfam* knock-down TECs. **(F)** Cellular ATP content normalized to total protein of control and *Tfam* knock-down TECs.

Supplementary Figure 4 (Related to Figure 4)



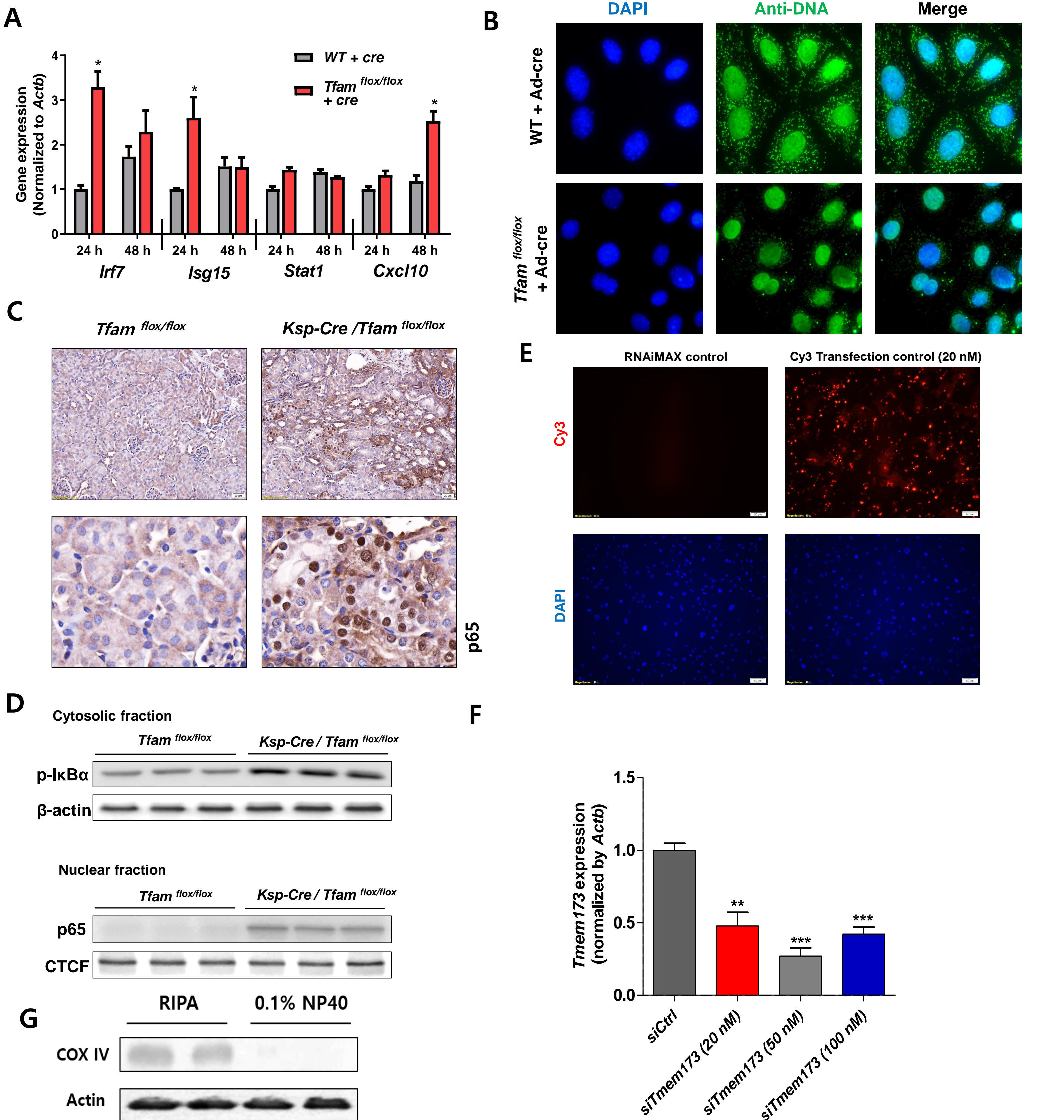
Supplementary Figure 4 (Related to Figure 4). Expression of mitochondrial genes in *Ksp-Cre/Tfam*^{flox/flox} mice. (A) Ki67 staining of 9 weeks old control WT and *Ksp-Cre/Tfam*^{flox/flox} mice. (B) Representative images of TUNEL staining in primary cultured cells treated with or without Cre adenovirus at 48 and 96 hrs. Scale bar = 10 μ m. (C) Heatmap of gene expression from RNAseq dataset. (D) RNA-sequencing was performed on kidneys of 12-week-old control ($n = 3$ WT/*Tfam*^{flox/flox}) and *Ksp-Cre/Tfam*^{flox/flox} ($n = 3$) mice. Gene ontology analysis (DAVID) of the differentially expressed genes in TFAM deficient mice. The graph shows $-\log P$ values calculated using modified Fisher Exact Test of a specific pathway. Relative gene expression of mitochondrial-encoded (E) or (F) nuclear-encoded mitochondrial genes in 12 week old control and *Ksp-Cre/Tfam*^{flox/flox} mice (G) Gene set enrichment analysis of the differentially expressed genes highlighting strong enrichment for the immune system process and metabolic process in samples.

Supplementary Figure 5 (Related to Figure 4)



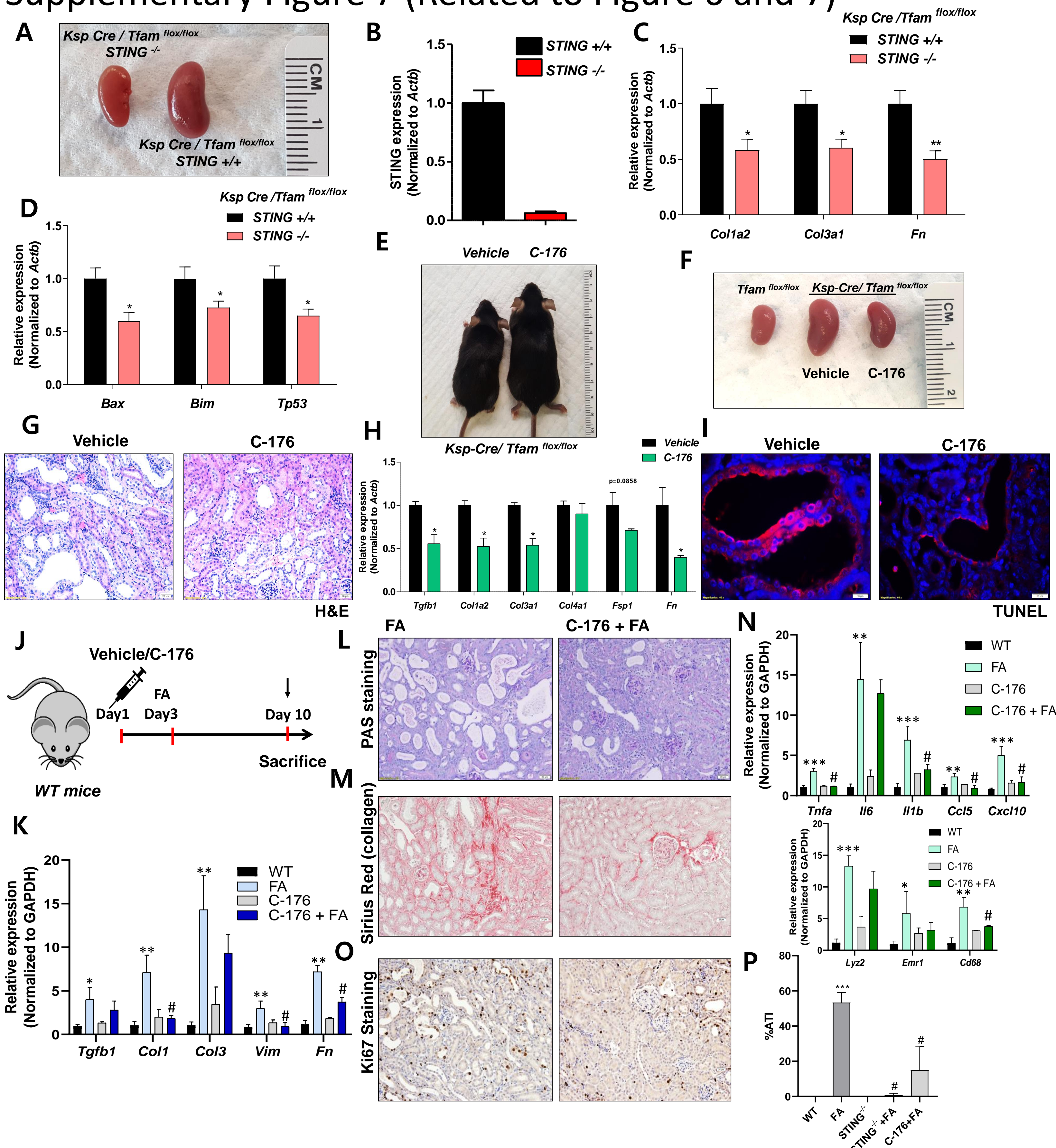
Supplementary Figure 5 (Related to Figure 4). Expression of inflammatory genes in control and *Ksp-Cre/Tfam^{flox/flox}* mice. (A) Relative mRNA levels of inflammatory cell marker genes (*Lyz2*, *Emr1*, and *Cd68*) of 6 weeks, 9 weeks and 12 weeks old *Ksp-Cre/Tfam^{flox/flox}* mice vs *WT/Tfam^{flox/flox}* mice. * $P < 0.05$ vs. 6 weeks *WT/Tfam^{flox/flox}*. * $P < 0.05$ vs. 9 weeks *WT/Tfam^{flox/flox}*. # $P < 0.05$ vs. 12 weeks *WT/Tfam^{flox/flox}*. (B) Heatmap of gene expression (from RNAseq) of NF-κB and IRF3 target genes (C) Expression of NF-κB and (D) IRF family genes (E) and NF-κB and IRF target genes in control and *Ksp-Cre/Tfam^{flox/flox}* mice. (F) Representative images of double staining by in situ hybridization with *Emr1* (red) and *Col1a2* (Green) probe in *Tfam*-deficient kidney cortex and medulla. Scale bar = 10 μm.

Supplementary Figure 6 (Related to Figure 5)



Supplementary Figure 6 (Related to Figure 5). TFAM loss in TECs induces cytokine expression via the activation of cGAS-STING pathway (A) Relative mRNA levels of IFN response genes (*Irf7*, *Isg15*, *Stat1*, and *Cxcl10*) in *Tfam*-deficient TECs. * $P < 0.05$. **(B)** Representative immunofluorescence images of control and *Tfam* knock-out TECs, stained with DAPI and anti-DNA antibody. Scale bar = 10 μ m. **(C)** Representative images of p65 immunostaining of control and *Ksp-Cre/Tfam*^{flox/flox} mouse kidneys. **(D)** Cytosolic protein levels of phosphorylated I κ B α and nuclear p65 levels in primary culture of control and *Tfam*-null TECs. **(E)** Transfection efficiency showed by Cy3 transfection control. **(F)** Relative *Tmem173* transcript level in primary TEC cells transfected with control siRNA and 20, 50 or 100 nM of siTmem173. **(G)** Immunoblotting of cytosolic fractions prepared 1% or 0.1% of NP40 with COX IV to confirm the lack of cross contamination with membrane fractions.

Supplementary Figure 7 (Related to Figure 6 and 7)



Supplementary Figure 7 (Related to Figure 6 and 7). Genetic deletion or pharmacological inhibition of STING attenuates renal disease of TFAM-deficient kidneys. (A) Gross kidney morphology of *Ksp-Cre/Tfam^{flox/flox}* and *Ksp-Cre/Tfam^{flox/flox}STING^{-/-}* mice (B) Relative mRNA levels of *STING*, (C) profibrotic genes (*Col1a2*, *Col3a1*, *Fn*) and (D) apoptosis-associated genes (*Bax*, *Bim*, *Tp53*) in *Ksp-Cre/Tfam^{flox/flox}* and *Ksp-Cre/Tfam^{flox/flox}STING^{-/-}* mice (E) Representative pictures of the mice and (F) kidneys of *Ksp-Cre/Tfam^{flox/flox}* mice treated with C-176/vehicle. * $P < 0.05$ vs. vehicle treated mice, # $P < 0.05$ vs. vehicle treated mice. (G) Representative images showing H&E staining of 12 weeks old *Ksp-Cre/Tfam^{flox/flox}* mice treated with C-176 or vehicle. (H) Relative mRNA levels of profibrotic genes levels (*Tgfb1*, *Col1a2*, *Col3a1*, *Col4a1*, *Fsp1*, *Fn*) in *Ksp-Cre/Tfam^{flox/flox}* mice treated with C-176 or vehicle. * $P < 0.05$ vs. vehicle treated mice. (I) Representative images showing TUNEL staining of 12 weeks old *Ksp-Cre/Tfam^{flox/flox}* mice treated with C-176 or vehicle. (J) Experimental scheme: WT mice were injected with STING inhibitor (C-176)/vehicle intraperitoneally every day and treated with single dose of folic acid (250mg/kg body weight) or vehicle on day 3. Mice were euthanized on day 10 (7 days post FA injection) ($n = 3$). (K) Relative mRNA of pro-fibrotic genes (*Tgfb1*, *Col1*, *Col3*, *Vim*, and *Fn1*). * $P < 0.05$, ** $P < 0.01$ vs. *Wt*. # $P < 0.01$ vs. FA mice (L) Representative images of PAS stained (M) Sirius red (O) Ki67 staining of FA-injected and C-176 + FA-injected mice kidney. Scale bar = 20 μ m. (N) Relative mRNA of proinflammatory cytokines (*Tnfa*, *Il1b*, *Il6*, *Ccl5* and *Cxcl10*) and immune cell markers (*Lyz2*, *Emr1*, *Cd68*) in mice injected with FA and C-176 + FA. ** $P < 0.01$ vs. WT. # $P < 0.01$ vs. FA mice. (P) STING activity ablation reduced the acute tubular injury score. *** $P < 0.001$ vs. WT. # $P < 0.01$ vs. FA mice.